Molecular Dynamics Simulation Studies of Physico Chemical Properties of Liquid Pentane Isomers

Seng Kue Lee and Song Hi Lee*

Department of Chemistry, Kyungsung University, Pusan 608-736, Korea
Received January 15, 1999

We have presented the thermodynamic, structural and dynamic properties of liquid pentane isomers - normal pentane, isopentane, and neopentane - using an expanded collapsed atomic model. The thermodynamic properties show that the intermolecular interactions become weaker as the molecular shape becomes more nearly spherical and the surface area decreases with branching. The structural properties are well predicted from the site-site radial, the average end-to-end distance, and the root-mean-squared radius of gyration distribution functions. The dynamic properties are obtained from the time correlation functions - the mean square displacement (MSD), the velocity auto-correlation (VAC), the cosine (CAC), the stress (SAC), the pressure (PAC), and the heat flux auto-correlation (HFAC) functions - of liquid pentane isomers. Two self-diffusion coefficients of liquid pentane isomers calculated from the MSD's *via* the Einstein equation and the VAC's *via* the Green-Kubo relation show the same trend but do not coincide with the branching effect on self-diffusion. The rotational relaxation time of liquid pentane isomers obtained from the CAC's decreases monotonously as branching increases. Two kinds of viscosities of liquid pentane isomers calculated from the SAC and PAC functions *via* the Green-Kubo relation have the same trend compared with the experimental results. The thermal conductivity calculated from the HFAC increases as branching increases.

Introduction

The family of organic compounds called hydrocarbons can be divided into several groups based on the type of bond that exists between the individual carbon atoms. Those hydrocarbons in which all the carbon-carbon bonds are single bonds are called alkanes. They have the general formula, C_nH_{2n+2}. Straight chain alkanes are called normal alkanes, or simply *n*-alkanes. The straight chain alkanes constitute a family of hydrocarbons in which a chain of $-CH_2-$ groups is terminated at both ends by a hydrogen and they have the general formula, $H-(CH_2)_n-H$.

Normal pentane is an example of straight chain alkanes. One glance at its three-dimensional structure shows that because of the tetrahedral carbon atoms their chains are zigzagged and completely straight. Indeed, the structure is the straightest possible arrangements of the chains, for rotations about the carbon-carbon single bonds produce arrangements that are less straight. The better description is unbranched. This means that each carbon atom within the chain is bonded to no more than two other carbon atoms and that unbranched alkanes contain only primary and secondary carbon atoms.

Isopentane and neopentane are examples of branched chain alkanes. In neopentane the central carbon atom is bonded to four carbon atoms. Normal pentane, isopentane and neopentane have the same molecular formula: C_5H_{12}. In three compounds, the atoms are connected in a different order. They are, therefore, constitutional isomers.[1] The three geometries of pentane isomers are shown in Figure 1.

The physical properties of the alkanes follow the pattern laid down by methane and are consistent with the alkane structure.[2] An alkane molecule is held together entirely by covalent bonds. Those bonds either join two atoms of the same kind and hence are non-polar, or join two atoms that differ very little in electronegativity and hence are only slightly polar. Furthermore, these bonds are directed in a very symmetrical way, so that the slight bond polarities tend to cancel out. As a result an alkane molecule is either non-polar or very weakly polar.

The forces holding non-polar molecules together (van der Waals force) are weak and effective in a very short range. They act only between the portions of different molecules that are in close contact, that is, between the surfaces of molecules. Therefore one would expect that within a family, the larger the molecule, and hence the larger its surface area, the stronger the intermolecular forces. Thus, the boiling and melting points of liquid alkanes rise as the number of carbon atoms increases. Boiling and melting require overcoming the intermolecular forces of a liquid or solid. Branched chain hydrocarbons are more compact than their straight chain isomers. For this reason, branched hydrocarbons tend to have lower boiling points and higher densities than their straight chain isomers.

Constitutional isomers have different physical properties, although they have the same carbon number. The difference may not be large, but they have different melting points, boiling points, densities, indexes of refraction, and so forth. As mentioned above a branched chain hydrocarbon has a lower boiling point than its straight chain isomer. Thus normal pentane has a boiling point of 36 °C, isopentane with a single branch 28 °C, and neopentane with two branches 9.5 °C. The effect of branching on boiling point is observed within all families of organic compounds. It is reasonable that branching should lower the boiling point: with branch-

ing the molecular shape tends to approach that of a sphere, and as this happens the surface area decreases, as a result the intermolecular forces become weaker and are overcome at a lower temperature.

In the present paper, we perform equilibrium molecular dynamics simulations to investigate the thermodynamic, structural, and dynamic properties and to calculate transport coefficients, namely the self-diffusion coefficient D_s, the shear viscosity η, the bulk viscosity κ, and the thermal conductivity λ, of liquid pentane isomers at 273.15 K using an expanded collapsed atomic model. The model includes C-C bond stretching and C-C-C bond angle bending potentials in addition to Lennard-Jones potential and C-C-C-C torsional rotational potential.

In Section II we present the molecular models and molecular dynamics simulation method. We discuss our simulation results in Section III and present concluding remarks in Section IV.

Molecular Models and Molecular Dynamics Simulations

The expanded collapsed atomic model includes the C-C bond stretching and C-C-C bond angle bending potential in addition to the Lennard-Jones (LJ) and torsional rotational potentials of the original Rykaert Bellemans' (RB) collapsed atomic model:[3]

$$V_b(r_{ij}) = K_0(r_{ij} - r_e)^2 \quad (1)$$

$$V_a = K_1(\theta - \theta_e)^2 - K_2(\theta - \theta_e)^3 \quad (2)$$

The equilibrium bond length (r_e) is fixed at 1.53 Å and the bond angles (θ_e) are also fixed, at 109.47 degrees. The force constants (K_0, K_1, and K_2) are those used by Lee *et al.*[4] and Chynoweth *et al.*,[5-7] which were originally provided by the work of White and Boville.[8] They are given in Table 1.

In the original RB model,[3] monomeric units are treated as single spheres, with their masses given in Table 2. They interact through an LJ potential between the spheres in different molecules and between the spheres more than three places apart on the same molecule. The C-C-C-C torsional rotational potential is given as

$$V(\phi) = c_0 + c_1\cos\phi + c_2\cos^2\phi - c_3\cos^3\phi + c_4\cos^4\phi + c_5\cos^5\phi \quad (3)$$

where ϕ is the C-C-C-C dihedral angle. The Lennard-Jones parameters and c_i values are listed in Table 1. Unlike in normal pentane, there are multiply imposed torsional rotational potentials in isopentane. That is to say, one doubly imposed dihedral state on the C_2-C_3 bond in isopentane exists as shown in Figure 1.

The molecular dynamics simulation parameters such as number of molecules, mass of site, temperature, and length of simulation box are listed in Table 2. The density of isopentane at 273.15 K is not widely reported in the literature; therefore, it is inferred from the known densities at other temperatures - 0.62473 at 288.15 K, 0.61972 at 293.15 K, and 0.61455 at 298.15 K. The usual periodic boundary condition in the x-, y-, and z- directions and minimum image convention for pair potential were applied. A spherical cut-off of radius $R_c = 2.5\sigma$, where σ is the Lennard-Jones parameter, was employed for the pair interactions. Gaussian isokinetics[9] was used to keep the temperature of the system constant.

Table 1. Potential parameters for liquid pentane isomers

LJ parameters	σ (nm)			ε (kJ/mol)	
C-C	0.3923			0.5986	
torsional	c_0(kJ/mol)	c_1	c_2	c_3	c_4	c_5
C-C-C-C	9.279	12.156	-13.120	-3.060	26.240	-31.495
bond stretching	r_e (nm)			K_0(kJ/mol · nm^2)	
C-C	0.153			132600	
bond angle bending	θ_e (deg)		K_1(kJ/mol · deg^2)	K_2(kJ/mol · deg^3)	
C-C-C	109.47		0.05021	0.000482	

Table 2. Molecular dynamics simulation parameters for model of liquid pentane isomers

Pentane isomers	Number of molecules	Mass of site (g/mole)	Temperature (K)	Density (g/cc)	Length of box (nm)
n-pen	64	14.42996	273.15	0.645	2.2823
i-pen	64	14.42996	273.15	0.639	2.2894
neo-pen	64	14.42996	273.15	0.613	2.3213

For the integration over time, we adopted Gear's fifth order predictor-corrector algorithm[10] with a time step of 0.0005 ps. MD runs of about 1,000,000 time steps were needed for each liquid pentane isomer system to reach equilibrium. The equilibrium properties were then averaged over 10 blocks of 100,000 time steps for a total of 1,000,000 time steps, and the configurations of molecules were stored every 10 time steps for analyses of structural and dynamic properties. As the systems approached the equilibrium states, the molecules were moving continually in the simulation box. The transport properties of liquid pentane isomers were cal-

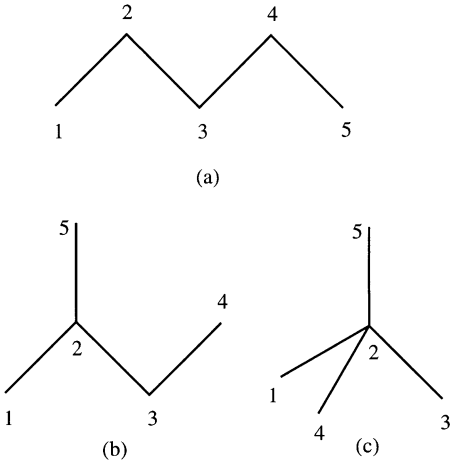

Figure 1. Geometries of (a) normal pentane, (b) isopentane, and (c) neopentane.

culated using the Green-Kubo relations[11-14] of the various correlation functions as given in Section III. The integrands in Eqs. (5), (7), (10), (13), and (16) are called the velocity, the cosine, the stress, the pressure, and the heat flux autocorrelation functions, respectively.

Results and Discussion

Thermodynamic properties. Thermodynamic and structural properties of the expanded collapsed atomic model for liquid normal pentane (*n*-pen), isopentane (*i*-pen), and neopentane (*neo*-pen) are listed in Table 3.

The molecular temperatures for liquid pentane isomers held at about 273.15 K. The atomic temperatures were lower than the molecular temperatures, which means that the atomic activity in pentane isomers is less than that in the monatomic system, probably due to the C-C and C-C-C potentials. The pressure decreases as branching increases (263.4 + 283.8/76.7 + 276.9/−151.4 + 250.5). The inter C-C LJ energy negatively decreases as branching increases, which reflects weaker intermolecular interactions as the molecular shape approaches a sphere, with the surface area decreasing with branching. Note that there is no intra C-C LJ potential for isopentane and neopentane.

The C-C bond stretching and C-C-C bond angle bending energies show other branching effects. As the molecular shape approaches that of a sphere, the steric effect becomes large and the monomeric units repel each other, which contributes the large repulsive interactions of the bond stretching and the bond angle bending potential energies. So C-C-C bond angle bending potential energy for neopentane is the largest, with that of isopentane the second largest. The behaviour of C-C bond stretching energies, however, is different from that of C-C-C bond angle bending energies: the C-C bond stretching for neopentane is smaller than normal pentane and isopentane since the C-C bond stretching in neopentane is independent of each other.

Table 3. Thermodynamic and structural properties for liquid pentane isomers

properties	*n*-pen	*i*-pen	*neo*-pen
molecular temperature (K)	273.2±2.3	273.2±2.3	273.2±2.0
atomic temperature (K)	240.9±17.7	251.5±18.7	223.9±15.9
pressure (atm)	263.4−283.8	76.7±276.9	-151.4±250.5
inter C-C LJ energy (kJ/mol)	-24.46±0.40	-23.36±0.37	-21.61±0.34
intra C-C LJ energy	-0.46±0.40	-	-
C-C-C-C torsional energy	2.173±0.232	2.371±0.125	-
C-C stretching energy	2.547±0.307	3.265±0.383	2.275±0.264
C-C-C angle bending energy	3.312±0.418	4.211±0.485	4.886±0.514
average % of C-C-C-C *trans*			
1st	73.97±4.94	51.54±1.32	-
2nd	72.87±5.56	36.88±1.81	-
total barrier crossing T-G	1920/2000.000	13/2000.000	-
G-T	1917/2000.000	12/2000.000	-
av. ene-to-end distance (nm)	0.4633±0.0043	0.3332±0.0010	0.2495±0.0003
rms radius of gyration	0.1741±0.0011	0.1508±0.0003	0.1367±0.0019

Normal pentane and isopentane have two dihedral states as shown in Figure 1: 1-2-3-4 and 2-3-4-5 in normal pentane, and 1-2-3-4 and 5-2-3-4 in isopentane. But there is one doubly imposed torsional rotational potential on the bond of 2-3 in isopentane, and the dihedral states of 1-2-3-4 and 5-2-3-4 are almost fixed as shown in the total barrier cross T-G and G-T. The average % of C-C-C-C *trans* and the total barrier cross T-G and G-T in isopentane are related to the doubly imposed dihedral state in the way that if the dihedral state of 1-2-3-4 is in *trans*, then that of 5-2-3-4 should be in *gauche*, or vice versa. Theoretically, the average % of C-C-C-C *trans* in isopentane is 50%, although not exactly 50% in this study. The average % of C-C-C-C *trans* of the expanded collapsed atomic model for branched-chain alkanes are generally greatly increased and the total barrier crossing T-G and G-T are largely decreased compared with those of the straight chain alkanes due to the doubly imposed dihedral state. Our results for the total barrier crossing T-G and G-T are in agreement with these observations. The root-mean-squared (rms) radius of gyration and average end-to-end distance decreases as branching increases due to the molecular shape.

Structural properties. The site-site radial distribution function, $g(r)$, the average end-to-end distance distribution function, and the root-mean-squared radius of gyration distribution function for liquid pentane isomers are shown in Figures 2, 3, and 4, respectively. The sharp peaks in the $g(r)$ functions are due to the contribution from intramolecular sites, while the smooth peaks come from intermolecular sites.

In Figure 2, normal pentane has two peaks, corresponding to *gauche*(G) and *trans*(T), and the broad curve corresponds to the contribution from intermolecular sites. But because there is no the rigidity of C-C bond length and C-C-C bond angle in this model, the $g(r)$ have relatively lower peaks. The $g(r)$ of normal pentane shows the contribution of TT at r^*=1.26, where $r^*=r/\sigma$, and between these sharp peaks there

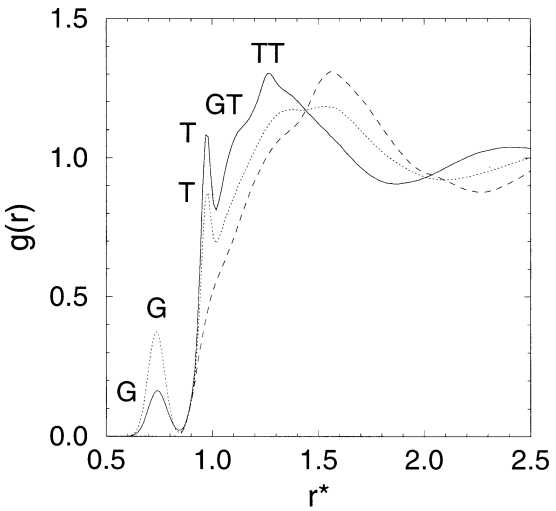

Figure 2. Site-site radial distribution function for liquid pentane isomers, normal pentane (—), isopentane (···), and neopentane (– –). $r^*=r/\sigma$.

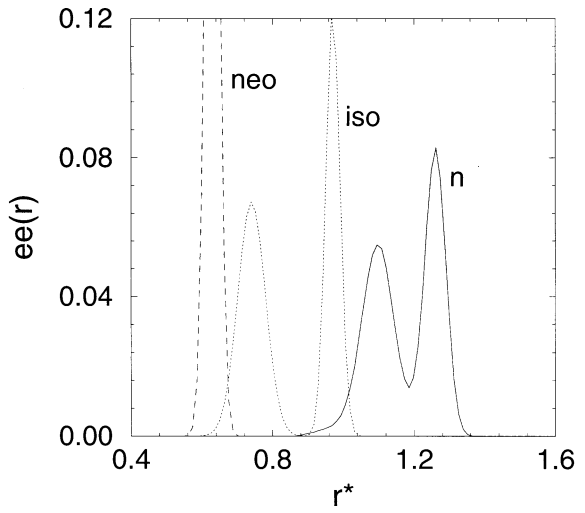

Figure 3. Average end-to-end distance distribution for liquid pentane isomers, normal pentane (—), isopentane (···), and neopentane (– –). $r^*=r/\sigma$.

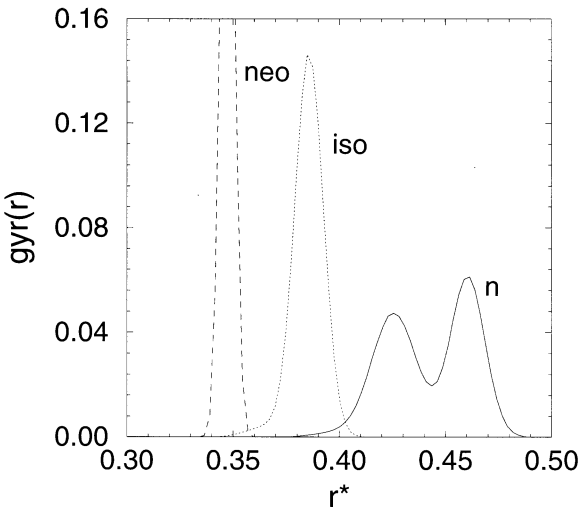

Figure 4. Root-mean-squared radius of gyration distribution for liquid pentane isomers, normal pentane (—), isopentane (···), and neopentane (– –). $r^*=r/\sigma$.

are somewhat broad curves corresponding to the contribution of TG (or GT) between T and TT at about r^*−1.04. The exact end-to-end distance of the TG conformation is r^*−1.04.[4] The contribution of GG is very small and does not appear in the $g(r)$ since the average % of GG is 7.13%.

The $g(r)$ of isopentane shows different behavior compared with that of normal pentane. There are no peaks corresponding to the contributions of TT and TG conformations. But the two peaks corresponding to G and T appear. The peak corresponding to G in isopentane is much higher than that in normal pentane due to the doubly imposed dihedral state in isopentane. The average % of *gauche* are 47.44 and 26.72, respectively.

The $g(r)$ of neopentane is much different from that of normal pentane and isopentane. The $g(r)$ of neopentane is contributed only from intermolecular site at r^*−1.85-2.50. If the contribution from intramolecular sites is removed from Figure 2, the curves move toward larger r^* as branching increases. This implies that the molecular shape tends to approach that of a sphere, with the surface area decreasing and the intermolecular interaction becoming weaker as seen in the inter C-C LJ energy. As a result, the distances between the intermolecular sites are larger as branching increases.

In Figure 3, we show the average end-to-end distance distribution functions for liquid pentane isomers as a function of r^*. For normal pentane, the lower peak at r^*−1.09 comes from the TG (or GT) conformation at exactly r^*−1.04 and the higher peak at about r^*−1.26 is from the TT conformation at an end-to-end distance r^*−1.35. For isopentane, the lower peak at about r^*−0.73 comes from *gauche* conformation at the exact end-to-end distance r^*−0.65, and the higher peak at about r^*−0.96 come from the *trans* at the exact end-to-end distance r^*−0.98. The end-to-end distance distribution function for isopentane is very similar to that of normal butane.[4] But there is no contribution corresponding to *gauche* and *trans* in the case of neopentane, and so there is only one high peak.

The distributions of root-mean-squared radius of gyration for liquid pentane isomers are displayed in Figure 4, and they have the same features as those of the average end-to-end distance distribution except for isopentane. In the case of isopentane, two distinct peaks of the average end-to end distance distribution do not appear in the root-mean-squared radius of gyration distribution due to the molecular shape of isopentane, *i.e.*, due to the doubly imposed dihedral state.

Dynamic properties. The mean square displacements (MSD) obtained from our MD simulation for liquid pentane isomers are shown in Figure 5. The MSD's for neopentane and isopentane in the figure are nearly in distinguishable. The self-diffusion coefficients for liquid pentane isomers calculated from MSD's using the Einstein relation:

$$D_s=\frac{1}{6}\lim_{t\to\infty}\frac{d\langle|\boldsymbol{r}(t)-\boldsymbol{r}(0)|^2\rangle}{dt} \tag{4}$$

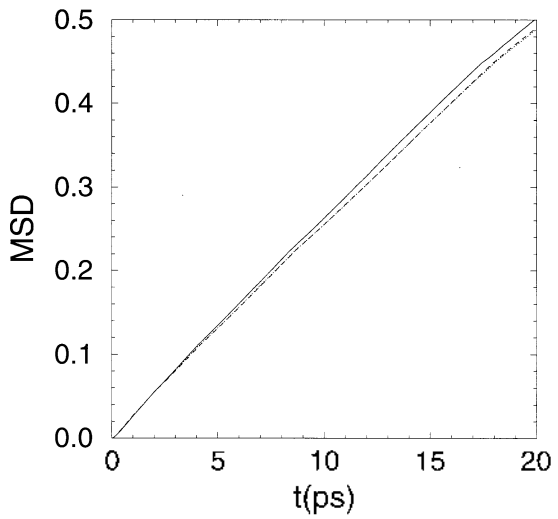

Figure 5. Mean square displacement as a function of time for liquid pentane isomers, normal pentane ( ), isopentane (···), and neopentane (– –).

Table 4. Self-diffusion coefficients (D_s, 10^{-9} m²/s) for liquid pentane isomers calculated from MSD

pentane isomers	D_s
n-pen	4.140±0.028
i-pen	4.014±0.037
neo-pen	4.041±0.034

are listed in Table 4. The calculated self-diffusion coefficients of neopentane and isopentane are nearly the same within statistical error. The self-diffusion coefficient of normal pentane is much larger than those of the other two isomers. In the Green-Kubo equation for the velocity auto-correlation function (VAC), the self-diffusion coefficient can be separated into two parts according to:

$$D_s=\frac{1}{3}\int_0^\infty \langle v(0)\cdot v(t)\rangle\, dt=\frac{1}{3}\langle v^2\rangle A, \tag{5}$$

where v is the velocity of particle, and the integration value of the normalized VAC function, A:

$$A=\int_0^\infty \frac{\langle v(0)\cdot v(\tau)\rangle}{\langle v(0)\cdot v(0)\rangle}d\tau. \tag{6}$$

The running integrals of the self-diffusion coefficient [Eq. (5)] from the velocity auto-correlation (VAC) functions for liquid pentane isomers are shown in Figure 6. The integral values of the self-diffusion coefficient for isopentane and neopentane in the figure are almost the same, as also seen in Figure 5 for MSD's. The self-diffusion coefficients for liquid pentane isomers calculated from the VAC using the Green-Kubo relation are slightly higher than those from the MSD as shown in Table 5 by 6-8%, but they show the same trend. The self-diffusion coefficients calculated from the two different routes are comparatively in good agreement but do not coincide with the branching effect on the self-diffusion property of liquid pentane isomers. This is a subtle and puzzling issue. As discussed in the thermodynamic properties of

Table 5. Self-diffusion coefficients (D_s, 10^{-9} m²/s) for liquid pentane isomers calculated from VAC. The value A(ps) is the integration value of Eq. (6) and kT/m in 10^3 m²/s²

pentane isomers	kT/m	A	D_s
n-pen	31.48±0.00	0.1385±0.0068	4.461±0.025
i-pen	31.48±0.00	0.1358±0.0072	4.263±0.038
neo-pen	31.48±0.00	0.1416±0.0065	4.274±0.026

liquid pentane isomers, the inter C-C LJ energy negatively decreases as branching increases, and, as discussed below, the shear and bulk viscosities decrease as branching increases, which a weakening of the intermolecular interactions as the molecular shape approaches that of a sphere and the surface area decreases with branching. And accordingly, the self-diffusion coefficients of liquid pentane isomers should increase monotonously as branching increases, but the calculated self-diffusion coefficients from MSD and VAC in our MD simulation does not follow this trend. The decrement of the inter C-C LJ energy and of the shear and bulk viscosities with increasing branching might be related to the rotational behaviour of the liquid pentane isomers rather than to the translational behaviour.

In Figure 7, the cosine auto-correlation(CAC) functions of liquid pentane isomers are plotted. The CAC function, $\langle\cos\theta(t)\rangle$, of rigid molecule is usually defined as

$$\langle\cos\theta(t)\rangle=\langle \boldsymbol{u}_X(0)\cdot\boldsymbol{u}_X(t)+\boldsymbol{u}_Y(0)\cdot\boldsymbol{u}_Y(t)+\boldsymbol{u}_Z(0)\cdot\boldsymbol{u}_Z(t)\rangle \tag{7}$$

where $\boldsymbol{u}_i$ is the direction vector of i component of molecular axis with unit magnitude, and $\theta(t)$ is the angle between the molecular axis and the z-axis at time t. In the this study the molecules of pentane isomers are not rigid and several unit vectors in each molecule are defined by joining vectors from the center of mass to the interaction sites of the molecule with unit magnitude. The CAC functions are calculated for each unit vector using Eq. (7) and averaged. Rotational relaxation time is defined by

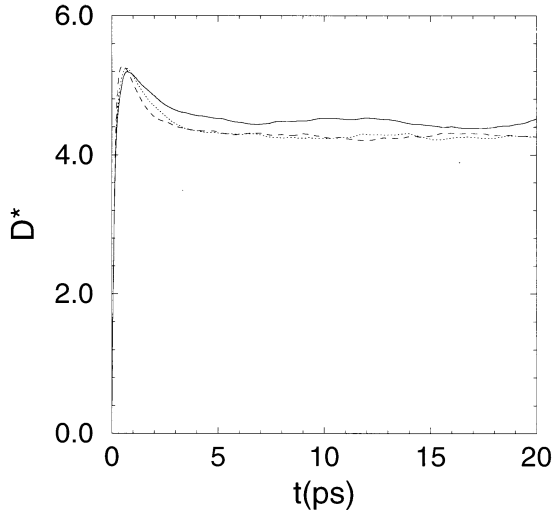

Figure 6. Running integral of the self-diffusion coefficient as a function of time [Eq. (5)] for liquid pentane isomers, normal pentane (—), isopentane (···), and neopentane (– –).

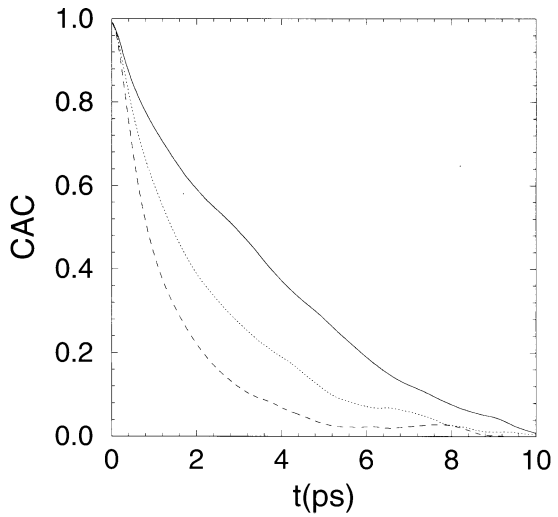

Figure 7. Cosine auto-correlation function for liquid pentane isomers, normal pentane (—), isopentane (···), and neopentane (– –).

Table 6. Rotational relaxation times (ps) for liquid pentane isomers calculated from Eqs. (8) and (9)

pentane isomers	τ [Eq. (8)]	τ [Eq. (9)]
n-pen	3.388(0-10.5)[a]	3.093(0-8.9)[b]
i-pen	2.209(0-10.8)	2.148(0-9.8)
neo-pen	1.885(0-9.3)	1.508(0-5.5)

[a]( ) are the time intervals (ps) of integration for Eq. (8). [b]( ) are the time intervals (ps) of exponential fitting for Eq. 9).

$$\tau=\int_0^\infty \langle \cos\theta(t)\rangle dt. \tag{8}$$

Table 6 shows the rotational relaxation times of liquid pentane isomers calculated from Eq. (8) and those obtained by fitting the CAC function to an exponential decay

$$\langle \cos\theta(t)\rangle \approx \exp((-t)/\tau), \tag{9}$$

which is especially useful when τ is large. The calculated τ's for liquid pentane isomers from the CAC functions through two routes, Eqs. (8) and (9), Which are nearly the same except for neopentane and show the same trend with increasing branching. The rotational relaxation time of liquid pentane isomers decreases monotonously as branching increases. This observation coincides with the branching effect on the rotation property of liquid pentane isomers. As the molecular shape approaches that of a sphere and the surface area decreases with branching, rotation of the molecule on the center of mass increases rapidly. This result of rotational relaxation time also coincides with the decrement of the inter C-C LJ energy, and the shear and bulk viscosities with increasing branching. The rotational behavior of the liquid pentane isomers has no correlation with the translational behavior. Combining the rotational behavior with the self-diffusion behavior discussed above, we can see that the normal pentane molecule moves snake-like and the other two isomers rotate more easily with less translational displacements than the normal pentane. A similar effect caused by branching on self-diffusion is observed in the equilibrium molecular dynamics studies of liquid C_{17} alkanes - normal heptadecane, 6-pentyl duodecane, and 5-dibutyl nonane.[4,15,16] The inter C-C LJ energy negatively decreases (−96.39, −76.18, and −68.46 kJ/mol) and the self-diffusion coefficient calculated from MSD is decreases (1.30, 1.10, and 0.833×10^{-9} m^2/s) as branching increases. The same trend is observed for liquid C_4 alkanes - *n*-butane and *i*-butane (−17.66 and −17.25 kJ/mol: 7.83 and 3.54×10^{-9} m^2/s), but not for liquid C_{10} alkanes - *n*-decane and 4-propyl heptane (−52.96 and −44.22 kJ/mol: 2.53 and 2.61×10^{-9} m^2/s). The rotational behavior of these alkane systems on increased braching was not investigated.

The Green-Kubo relation for the shear viscosity, η, is given by the integral of the stress auto-correlation function (SAC):

$$\eta=\frac{V}{kT}\int_0^\infty \langle P_{xy}(p)\ P_{xy}(t)\rangle dt, \tag{10}$$

where P_{xy} is an off-diagonal ($x \neq y$) of the viscous pressure tensor. The alternative method proposed by Evans[17] and derived using the principles of linear-irreversible thermodynamics,[18,19] takes advantage of the isotropic symmetry but makes use of the full pressure tensor, which allows for improved statistics. This generalized Green-Kubo relation for the shear viscosity is also separated into two parts according to:

$$\eta=\frac{V}{10kT}\int_0^\infty \langle Tr[\tilde{P}(0)\tilde{P}(t)]\rangle\ dt=\frac{V\langle\tilde{P}^2\rangle}{10kT}B. \tag{11}$$

whererm $\tilde{P}$ is the symmetric traceless part of the full pressure tensor, and the integration value of the normalized SAC function, B:

$$B=\int_0^\infty \frac{\langle\tilde{P}(0)\ \tilde{P}(\tau)\rangle}{\langle\tilde{P}(0)\ \tilde{P}(0)\rangle}d\tau. \tag{12}$$

The bulk viscosity, κ, is also separated into two parts according to:

$$\kappa=\frac{1}{VkT}\int_0^\infty \langle(p(0)V(0)-\langle pV\rangle)(p(t)V(t)-\langle pV\rangle)\rangle dt$$

$$=\frac{V}{kT}\int_0^\infty \langle Q(0)\ Q(t)\rangle dt=\frac{V\langle Q^2\rangle}{kT}B' \tag{13}$$

where

$$Q(t)=p(t)-\langle p(0)\rangle=\frac{1}{3}(P_{xx}(t)+P_{yy}(t)+P_{zz}(t))-\langle p(0)\rangle \tag{14}$$

and the integration value of the normalized PAC function, B':

$$B'=\int_0^\infty \frac{\langle Q(0)\ Q(\tau)\rangle}{\langle Q(0)\ Q(0)\rangle}\ d\tau \tag{15}$$

The running integral of the shear [Eq. (11)] and bulk viscosities [Eq. (13)] from the stress auto-correlation (SAC) functions and the pressure auto-correlation (PAC) functions for liquid pentane isomers are shown in Figures 8 and 9. The

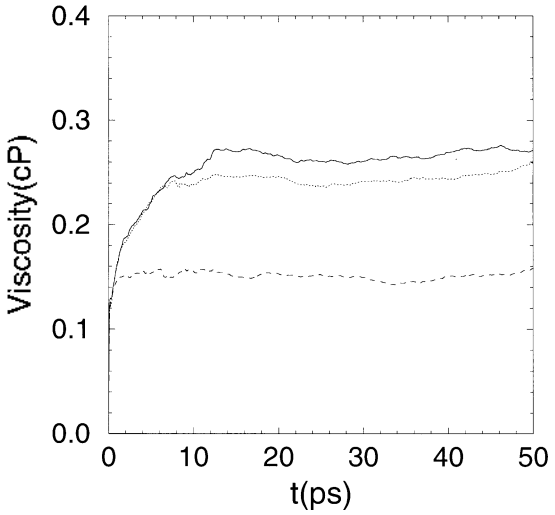

Figure 8. Running integral of the shear viscosity as a function of time [Eq. (11)] for liquid pentane isomers, normal pentane (—), isopentane (···), and neopentane (– –).

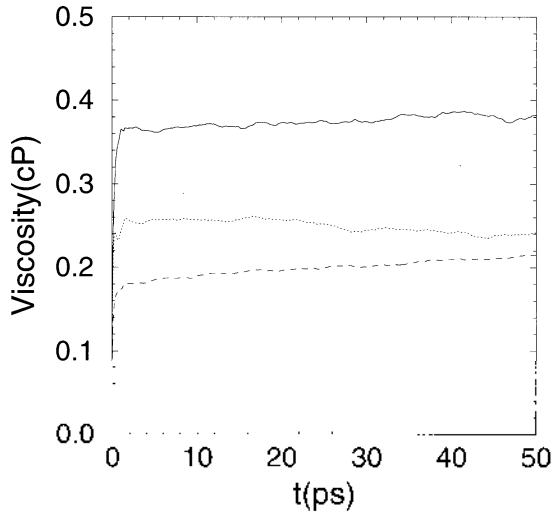

Figure 9. Running integral of the bulk viscosity as a function of time [Eq. (13)] for liquid pentane isomers. normal pentane(—), isopentane (···), and neopentane (– –).

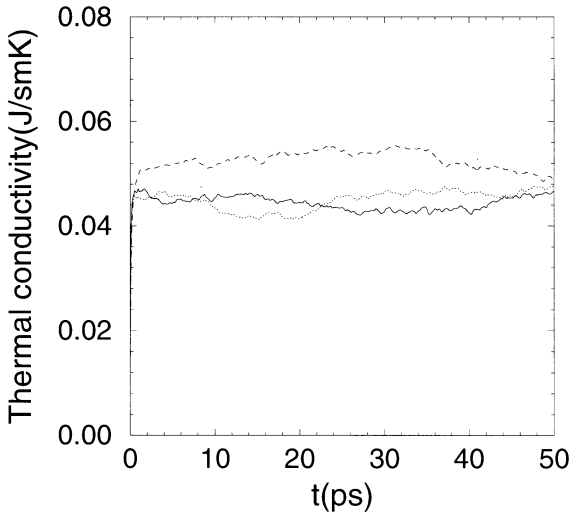

Figure 10. Running integral of the thermal conductivity as a function of time [Eq. (16)] for liquid pentane isomers. normal pentane ( ), isopentane (···), and neopentane (– –).

Table 7. Shear viscosities (η, cP) for liquid pentane isomers calculated from SAC. The value of B (ps) is the integration value of Eq. (12) and $V\langle\tilde{P}^2\rangle$/10kT in cP/ps

pentane isomers	$V\langle\tilde{P}^2\rangle$/10kT	B	η
n-pen	1.876±0.035	0.1422±0.0024	0.2667±0.0048
i-pen	1.634±0.037	0.1496±0.0025	0.2445±0.0048
neo-pen	1.325±0.027	0.1132±0.0021	0.1500±0.0032

Table 8. Bulk viscosities (κ, cP) for liquid pentane isomers calculated from PAC. The value of B' (ps) is the integration value of Eq. (15) and $V\langle Q^2\rangle$/kT in cP/ps

pentane isomers	$V\langle Q^2\rangle$/kT	B'	κ
n-pen	2.669±0.055	0.1406±0.0033	0.3752±0.0060
i-pen	2.367±0.048	0.1053±0.0038	0.2492±0.0076
neo-pen	2.076±0.068	0.0968±0.0031	0.2010±0.0081

shear viscosities and bulk viscosities calculated from the Green-Kubo relations are listed in Tables 7 and 8, respectively. The experimental viscosity of normal pentane at temperature 273.15 K is 0.289 cP and that of isopentane is 0.273 cP, and at 293.15 K 0.240 cP and 0.223 cP, respectively. Our results for the shear/bulk viscosities of normal pentane and isopentane calculated from the SAC and PAC functions at 273.15 K are (0.267 ± 0.005/0.375 ± 0.006) and (0.245 ± 0.005/0.249 ± 0.008), respectively. The agreement between the calculated shear viscosities and the experimental ones is very good for the two pentane isomers at 273.15 K. The non-equilibrium molecular dynamics (NEMD) results for the viscosity of liquid pentane isomers at 273.15 K[30] also give a very good agreement (0.26, 0.22, and 0.17 cP) with the present EMD result. Two kinds of viscosities for liquid pentane isomers calculated from the SAC and PAC function *via* the Green-Kubo relation show the same trend with the experimental results and this result coincides with the branching effect on the viscosity property of liquid pentane isomers. As the molecular shape approaches that of a sphere and the surface area decreases with branching, the viscosity of pentane isomers decreases. This result of the shear and bulk viscosities also coincides with the decrement of the inter C-C LJ energy and the rotational relaxation time with increasing branching.

The thermal conductivity, λ, is also separated into two parts according to:

$$\lambda=\frac{V}{3kT^2}\int_0^\infty \langle \boldsymbol{J}_Q(t)\cdot\boldsymbol{J}_Q(0)\rangle dt=\frac{V\langle J_Q^2\rangle}{3kT^2}C \tag{16}$$

where

$$\boldsymbol{J}_Q V=\sum_{i=1}^{N} E_i\boldsymbol{v}_i-\frac{1}{2}\sum_i\sum_j \boldsymbol{r}_{ij}(\boldsymbol{v}_i\cdot\boldsymbol{F}_{ij}) \tag{17}$$

and the integration value of the normalized HFAC function, C:

$$C=\int_0^\infty \frac{\langle \boldsymbol{J}_Q(0)\cdot\boldsymbol{J}_Q(\tau)\rangle}{\langle \boldsymbol{J}_Q(0)\cdot\boldsymbol{J}_Q(0)\rangle}d\tau \tag{18}$$

The running integral of the thermal conductivity [Eq. (16)] from heat-flux auto-correlation (HFAC) functions are shown in Figure 10. The thermal conductivities calculated from the Green-Kubo relation are listed in Table 9. The thermal conductivity calculated from the HFAC in our MD simulation increases as branching increases, and it shows a trend opposite to that of the shear and bulk viscosities and the rotational

Table 9. Thermal conductivities (λ, J/smK) for liquid pentane isomers calculated from HFAC. The value of C(ps) is the integration value of Eq. (18) and $V\langle J_Q^2\rangle$/3kT^2 in J/smKps

pentane isomers	$V\langle J_Q^2\rangle$/3kT^2	C	λ
n-pen	0.5830±0.0191	0.07611±0.00194	0.04437±0.00125
i-pen	0.5224±0.0105	0.08616±0.00162	0.04501±0.00188
neo-pen	0.4095±0.0147	0.12850±0.00218	0.05262±0.00277

relaxation times. But the detailed mechanism for the thermal conductivity of liquid pentane isomers is not fully understood.

Concluding Remarks

We have presented the results of thermodynamic, structural, and dynamic properties of liquid pentane isomers - normal pentane, isopentane, and neopentane - at 273.15 K, using an expanded collapsed atomic model.

The thermodynamic properties show that the intermolecular interactions become weaker as the molecular shape approaches that of a sphere and the surface area decreases with branching. The structural properties are well predicted from the site-site radial distribution function, the average end-to-end distance distribution function, and the root-mean-squared radius of gyration distribution function. In the case of isopentane, the root-mean-squared radius of gyration distribution function has a different behavior compared with the average end-to-end distance distribution function.

The dynamic properties are obtained from the time correlation functions - the mean square displacement, the velocity, the cosine, the stress, the pressure, and the heat flux autocorrelation functions - of liquid pentane isomers which are calculated from our MD simulations. Two self-diffusion coefficients of liquid pentane isomers calculated from the MSD's and the VAC's are comparatively in good agreement and show the same trend but do not coincide with the branching effect on the self-diffusion property of liquid pentane isomers. The rotational relaxation time of liquid pentane isomers obtained from the CAC's decreases monotonously as branching increases, which coincides with the branching effect on the rotation property of liquid pentane isomers. From the rotational and the self-diffusion behavior, it is observed that the normal pentane molecule moves snake-like and the other two isomers rotate more easily with less translational displacements than the normal pentane. Two kinds of viscosities of liquid pentane isomers calculated from the SAC and PAC functions *via* the Green-Kubo relation decrease as branching increases, which coincides with the branching effect on the viscosity property of liquid pentane isomers. The calculated shear viscosities of normal pentane and isopentane are in excellent agreement with the experimental results. The thermal conductivity calculated from the HFAC increases as branching increases, and it shows a trend opposite to that of the shear and bulk viscosities and the rotational relaxation times.

Conclusion

In conclusion, the overall agreement predicted by our MD simulations of liquid pentane isomers with the experimental data is quite good, which demonstrates the validity of our MD simulations for liquid pentane isomers are valid.

Acknowledgment. This research was supported by the Basic Science Research Institute Program, Ministry of Education (BSRI-97-3414). The authors would like to thank the Super Computer Center at the Electronics and Telecommunications Research Institute for access to its Cray-C90 super computer and the Tongmyung University of Information Technology for access to its IBM SP/2 computers. This research is a partial fulfillment of the requirements for the degree of Master of Science for Seng Kue Lee in Department of Chemistry, Graduate School, Kyungsung University.

References

1. Graham Solomon, T. W. *Organic Chemistry*, 4th ed.; John Wiley and Sons: New York, 1988.
2. Morrison, R. T.; Boyd, R. N. *Organic Chemistry*, 5th ed.; Allyn and Bacon: Boston, 1987.
3. Ryckaert, J. P.; Bellemans, A. *Discuss. Faraday Soc.* **1978**, *66*, 95.
4. Lee, S. H.; Lee, H.; Park, H.; Rasaiah, J. C. *Bull. Korean Chem. Soc.* **1996**, *17*, 735.
5. Chynoweth, S.; Klomp, U. C.; Scales, L. E. *Comput. Phys. Commun.* **1991**, *62*, 297.
6. Chynoweth, S.; Klomp, U. C.; Michopoulos, Y. *J. Chem. Phys.* **1991**, *95*, 3024.
7. Berker, A.; Chynoweth, S.; Klomp, U. C.; Michopoulos, Y. *J. Chem. Soc. Faraday Trans.* **1992**, *88*, 1719.
8. White, D. N. J.; Boville, M. J. *J. Chem. Soc., Perkin Trans.* **1977**, *2*, 1610.
9. Evans, D. J.; Hoover, W. G.; Failor, B. H.; Moran, B.; Ladd, A. J. C. *Phys.Rev.* **1983**, *A28*, 1016. (b) Simmons, A. J. D.; Cummings, P. T. *Chem. Phys. Lett.* **1986**, *129*, 92.
10. Gear, C. W. *Numerical Initial Value Problems in Ordinary Differential Equation*; Prentice-Hall: Englewood Cliffs, 1971.
11. Green, M. S. *J. Chem. Phys.* **1954**, 22, 398.
12. Kubo, R. *J. Phys. Soc. Jpn.* **1957**, *12*, 570.
13. Moon, C. B.; Moon, G. K.; Lee, S. H. *Bull. Korean Chem. Soc.* **1991**, *12*, 309.
14. Zwanzig, R. *Ann. Rev. Phys. Chem.* **1965**, *16*, 67.
15. Lee, S. H.; Lee, H.; Pak, H. *Bull. Kor. Chem. Soc.* **1997**, *18*, 478.
16. Lee, S. H.; Lee, H.; Pak, H. *Bull. Kor. Chem. Soc.* **1997**, *18*, 501.
17. Davis, P. J.; Evans, D. J. *J. Chem. Phys.* **1994**, *100*, 541.
18. Evans, D. J.; Morriss, G. P. *Statistical Mechanics of Non-equilibrium Liquids*; Academic: New York, 1990.
19. deGroot, S. R.; Mazur, P. *Non-equilibrium Thermodynamics*; Dover: New York, 1984.
20. Lee, S. H. submitted in *Mol. Sim.*